

Variability of lightning hazard over Indian region with respect to ENSO Phases

Avaronthan Veettil Sreenath¹, Sukumarapillai Abhilash^{1,2}, and Pattathil Vijaykumar^{1,2}

¹Department of Atmospheric Sciences, Cochin University of Science and Technology, Cochin 682016, India

²Advanced Department Centre for Atmospheric Radar Research, Cochin University of Science and Technology, Cochin 682022, India

Correspondence: S Abhilash (abhimets@gmail.com)

Abstract.

The El-Nino Southern Oscillation (ENSO) modulates the lightning flash rate (LFR) variability over India during pre-monsoon, monsoon, and post-monsoon seasons. This study intends to shed light on the impact of ENSO phases on the LFR over the Indian subcontinent using the data obtained from Optical Transient Detector (OTD) and Lightning Imaging Sensors (LIS) onboard the TRMM satellite. Results suggest that irrespective of ENSO phases, the LFR is maximum over northeast India (NEI) in the pre-monsoon season, and the peak is shifted to the north of northwest India (NNWI) in the monsoon season. The LFR over Northeast India (NEI) and southern peninsular India (SPI) strengthened (weakened) during the warm (cold) phase of ENSO in the pre-monsoon season. During monsoon season, NEI (NNWI) shows above normal LFR in the warm (cold) ENSO phase. It is striking to note that the three hotspots of LFR over the Indian land region became more prominent in the last decade of the monsoon season. A widespread increase of LFR is observed all over India during the warm phase of ENSO in the post-monsoon season. The subtropical westerly jet stream is shifted south in association with the warm phase, with an associated increase in the geopotential height (GPH) all over India in the same period. This exciting remark might explain the indirect influences of ENSO's warm phase on LFR during the post-monsoon season by pushing the mean position of subtropical westerly towards south latitudes. However, the marked increase of LFR is confined mostly over the NNWI in the cold ENSO phase.

1 Introduction

Lightning is a tremendous and inescapable atmospheric hazard that humankind has encountered throughout history (Cooray et al., 2007; Mills et al., 2010). For the 14 years from 2001 to 2014, the total number of deaths attributed to lightning hazards are 31725 over India (Selvi and Rajapandian, 2016). The number of casualties underlines lightning hazards as a devastating phenomenon, with an annual death rate of 2234 for the above period. Singh and Singh (2015) documented the yearly number of lightning fatalities and lightning flashes in India from 1998 to 2005, and they finds that the fatalities increase coherently with the lightning flash rate. Lightning strikes over the plain terrains are observed to be less as compared to the hilly regions. Due to the former's high population density, even lesser lightning flashes take many people's lives due to high chances of being struck by lightning (Yadava et al., 2020).

25 The El-Nino Southern Oscillation (ENSO) is a naturally occurring planetary-scale phenomenon related to the variations in
sea surface temperatures over the tropical Pacific Ocean, strongly influencing the number of flashes and average flash rate
(Kumar and Kamra, 2012). It is one of the most dynamic climatic variability modes, characterized by three phases: El-Nino
(Warm), La-Nina (Cold), and Neutral. The ENSO is a crucial player in the transport of heat, moisture, and momentum and
modulates the frequency, intensity, and location of deep convection and the associated lightning activity (Williams, 1992;
30 Kulkarni and Siingh, 2014). Higher Lightning Flash Rate (LFR) areas are located away from the equator during the warm
phase and coincide with regions of anomalous jet stream circulation enhanced by the meridional heat transport (Chronis et al.,
2008). Kandalgaonkar et al. (2010) has reported that lightning activity during the El-Nino year of 2002 increased by 18% over
the Indian land region compared to the La-Nina years during 1998-2011. On a global scale, lightning activity shows strong
regional preference during different ENSO Phases.

35 The changes in the lower and upper air circulations associated with different ENSO phases have been found to influence the
storm frequency and intensity (Yang et al., 2002; Hsu and Wallace, 1976), which in turn affect the lightning activity (Goodman
et al., 2000). Kent et al. (1995) observed that ENSO could dictate clouds' distribution over the tropics and subtropics. Owing
to the presence of anomalous subsidence over the western Pacific and adjacent landmass, deep convective clouds are inhibited;
hence the rainfall is less during the warm phase (Cess et al., 2001). A southward/eastward shift in the global lightning activity
40 is visible during the warm phase, and the latitudes corresponding to the descending limb of the Hadley circulation exhibit the
most significant contrast of LFR between the warm and cold phase of the ENSO (Sátori et al., 2009).

Generally, lightning activity is controlled by the clouds growing deep into the atmosphere. The deep convective cores present
over India's east coast during the pre-monsoon season shift to the foothills of western Himalayas during the monsoon (Ro-
matschke et al., 2010). Cecil et al. (2014) documented that India's offshore regions and the maritime continent are prone to
45 deep convection. The vertical growth of cloud systems is amplified by the intense updraft, promoting ice crystals and super-
cooled liquid (mixed-phase) inside the convective system. The interaction between these hydrometeors is mainly responsible
for the electrification inside the cloud (Takahashi et al., 1999; Williams, 2001). The atmosphere's dynamic and thermodynamic
states also modulate the lightning activity over a region (Williams, 1992; Zipser, 1994; Petersen et al., 1996; Rosenfeld, 1999).
Topography is also identified as a critical participant in developing deep convective clouds and impacts the distribution of
50 lightning activity (Kilinc and Beringer, 2007). Earlier studies have observed that elevated landmass favours the development of
deep convective clouds (Zipser et al., 2006; Houze Jr et al., 2007; Rasmussen and Houze Jr, 2011) and thereby leading to higher
LFR. Another agent that plays a decisive role in generating lightning activity is aerosols. Higher aerosol loading increases the
available liquid water in the mixed-phase condition, which is an essential factor for cloud electrification and lightning activity
(Williams et al., 2002). Venevsky (2014) reported a significant correlation between lightning and concentration of annually-
55 averaged cloud condensation nuclei over both land and ocean.

The awareness of lightning safety among the public is relatively low. The present study provides vital information on the
risky lightning periods over the Indian subcontinent and how the large scale phenomenon, ENSO, is influencing the same. We
are detailing the modulation of LFR under different ENSO phases with the help of a vertical profile of hydrometeors (graupel
and snow) inside the cloud systems and related atmospheric dynamics during pre-monsoon (March-May) monsoon (June-

60 September) and post-monsoon (October-December) seasons in India. The variability of LFR and hydrometeor distribution inside the convective system with different ENSO phases are very rare in the literature.

The organization of this paper is as follows. The datasets employed in this study are described in section 2. In section 3, we present the results followed by subsection 3.1, which depicts the composite analysis of LFR for pre-monsoon, monsoon, and post-monsoon seasons corresponding to the three ENSO phases. The remaining subsections of section 3 (3.2, 3.3 and 3.4) 65 portray the composite analysis of anomalous LFR during the different seasons and the significance of vertical cloud structure and associated dynamics in regulating their distribution. Finally, the conclusions of this work are given in section 4.

2 Data and methods

The Lightning Imaging Sensor (LIS) was an instrument onboard the Tropical Rainfall Measuring Mission (TRMM) satellite launched in December 1997. This instrument senses lightning flashes across the global tropics and subtropics (Goodman et al., 70 2007). The Optical Transient Detector (OTD) was the predecessor of LIS, launched in the MicroLab-1 satellite. Combined OTD (Optical Transient Detector) + LIS (Lightning Imaging Sensor) monthly averaged flash rates expressed flash km⁻²day⁻¹ available from <http://ghrc.nsstc.nasa.gov/> is used in this work. These products compute mean lightning flash rates by accumulating the total number of flashes observed and the entire observation duration for each grid box ($2.5^{\circ} \times 2.5^{\circ}$) from the thousands of individual satellite orbits. The lightning climatology derived from OTD / LIS (Cecil et al., 2014) provides a 75 unique observational basis for the global flash distribution in monthly time series (Kamra and Athira, 2016), seasonal cycles (Christian et al., 2003), or diurnal cycles (Blakeslee et al., 2014). To produce the low-resolution monthly time series (LMRTS) data, LIS and OTD flash rates and view times are smoothed precisely and are extracted for the middle day of each month (Cecil et al., 2014). The lightning flash rates in an LRMTS have slightly over three months of temporal smoothing and $7.5^{\circ} \times 7.5^{\circ}$ spatial smoothing (Cecil et al., 2014). The data sets are described in greater detail in the following paper: Gridded lightning 80 climatology from TRMM-LIS and OTD: Dataset description by Cecil et al. (2014).

The LFR data is available starting from July 1995 only. So the pre-monsoon season in our work starts in 1996 (March-May) and ends in 2013 (March-May). Due to data unavailability, the first monsoon season includes only three months (July, August, and September 1995). This particular season terminates in 2013 (June, July, August, and September). On the other hand, the post-monsoon season is prepared from 1995 (October-December) to 2013 (October-December). LFR anomaly in this study 85 indicates the difference between the composite of LFR during a particular ENSO phase in a specific season and the composite of LFR during all the three ENSO phases in that specific season. e.g., LFR anomaly during pre-monsoon during La-Nina = (Composite of LFR during La-Nina in pre-monsoon) - (Composite of LFR during all the three ENSO phases in pre-monsoon). The anomalies of all other parameters used in this study are calculated using the same method.

With the aid of TRMM-3A12 data, the cloud structure is examined by evaluating the vertical profiles of hydrometeors 90 (graupel, snow, rainwater) and latent heat release during different phases of ENSO. The data set has a spatial resolution of $0.5^{\circ} \times 0.5^{\circ}$, and it is available from January 1998 to December 2013. It has 28 vertical levels, which start from 0.5 km, and each level is separated by 0.5 km. Finally, the modulation of Geopotential height (GPH) at 500 hPa, wind at 200 hPa, and

| Year | Pre-monsoon | Monsoon | Post-monsoon |
|------|--------------|--------------|--------------|
| 1995 | <u>0.39</u> | <u>-0.08</u> | <i>-0.60</i> |
| 1996 | <u>-0.27</u> | <u>-0.10</u> | <u>-0.25</u> |
| 1997 | 0.51 | 1.81 | 2.41 |
| 1998 | 1.15 | <i>-0.57</i> | <i>-1.20</i> |
| 1999 | <i>-0.73</i> | <i>-0.77</i> | <i>-1.24</i> |
| 2000 | <i>-0.80</i> | <u>-0.39</u> | <i>-0.65</i> |
| 2001 | <u>-0.22</u> | <u>0.01</u> | <u>-0.25</u> |
| 2002 | <u>0.27</u> | 0.81 | 1.40 |
| 2003 | <u>0.10</u> | <u>0.15</u> | <u>0.46</u> |
| 2004 | <u>0.14</u> | 0.58 | 0.76 |
| 2005 | <u>0.41</u> | <u>0.14</u> | <u>-0.36</u> |
| 2006 | <u>-0.27</u> | <u>0.39</u> | 1.02 |
| 2007 | <u>-0.10</u> | <u>-0.40</u> | <i>-1.40</i> |
| 2008 | <i>-0.76</i> | <u>-0.08</u> | <u>-0.43</u> |
| 2009 | <u>-0.35</u> | 0.73 | 1.49 |
| 2010 | 0.62 | <i>-0.97</i> | <i>-1.52</i> |
| 2011 | <i>-0.61</i> | <u>-0.34</u> | <i>-0.96</i> |
| 2012 | <u>-0.17</u> | 0.53 | <u>0.21</u> |
| 2013 | <u>-0.03</u> | <u>0.39</u> | 0.79 |

Table 1. ONI during the pre-monsoon, monsoon, and post-monsoon season in India from 1995 to 2013. The bold, italics and underlined values denote El-Nino, La-Nina, and Neutral phases of ENSO, respectively.

specific humidity (SH) at 300 hPa are also examined with the ENSO phases from July 1995 to December 2013. The above parameters are obtained from the NCEP–National Center for Atmospheric Research (NCAR) reanalysis data with a similar spatial and temporal resolution of LFR. Oceanic Nino Index (ONI) is the standard used to identify different phases of ENSO. The average value of ONI is determined during pre-monsoon, monsoon, and post-monsoon season by using HadISST data and detailed in table 1. If the ONI value is above $+0.5^{\circ}$ (-0.5°) C, it is taken as the warm (cold) phase, and the neutral phase corresponds to the ONI index lies between $-0.5/+0.5^{\circ}$ C.

3 Results and discussion

3.1 Composite LFR with respect to ENSO phases

Figure 1 represents the LFR composites for pre-monsoon, monsoon, and post-monsoon seasons corresponding to the three ENSO phases. Irrespective of ENSO phases, the LFR peak is located over northeast India (NEI) during the pre-monsoon season, while its peak shifts to the north of northwest India (NNWI) in the monsoon season. Kamra and Athira (2016) have

previously reported a similar type of swing in LFR between pre-monsoon and monsoon seasons. The Himalayan orography
 105 favours the formation of deep convective systems over the NEI (Goswami et al., 2010) and is evidenced by the high values
 of LFR over the region. Rather than the altitude, the steep topographic gradient is responsible for producing deep convection.
 Most likely, the deep convective clouds developed in the conditionally unstable atmosphere during the pre-monsoon season
 are electrically more active (Williams et al., 1992). Lau et al. (2008) proposed that during the pre-monsoon months, dust and
 black carbon from neighbouring sources accumulates over the Indo-Gangetic plain against the foothills of the Himalayas and
 110 act as an elevated heat pump (EHP). Accordingly, this enhanced warming of the middle and upper troposphere contributes to
 the genesis of deep clouds and higher LFR.

Compared to monsoon and post-monsoon seasons, convective available potential energy (CAPE) is higher during the pre-
 monsoon season. The seasonal average of CAPE is highest over India's east coast, and it is near 1500 J/kg all over south India
 (Murugavel et al., 2014). Nevertheless, large regions of India, especially the central Indian region, show a seasonal average of
 115 CAPE less than 1000 J/Kg (Murugavel et al., 2014). Strikingly, the areas of higher values of LFR (Figure 1) during the pre-
 monsoon season coincide with the regions of CAPE maxima reported by (Murugavel et al., 2014). Previous works ascertain
 that the moderate updrafts limit the vertical development of convective clouds during the summer monsoon under the influence
 of maritime air mass (Kumar et al., 2014; Tinmaker et al., 2015), which leads to a decline in the cloud electrification during the
 monsoon season. Among the three seasons, post-monsoon shows a minimum of LFR over the Indian region (Figure 1), and the
 120 NW to the NE gradient of LFR is also observed to be weak in this season. One possible reason for this is the existence of a low
 average value of CAPE (<500 J/kg) over most parts of India during this season (Murugavel et al., 2014), which is relatively
 low to favour the development of deep convection and hence lightning.

3.2 Distribution of anomalous LFR during pre-monsoon season with respect to ENSO phases

Ahmad and Ghosh (2017) reported that compared to other Indian regions, lightning activity is higher over the North-Eastern
 125 part and southern part of India during the pre-monsoon season. They also observed that the maxima of lightning during post-
 monsoon is also lying over India's southern and eastern regions. Kamra and Athira (2016) identified a higher concentration of
 LFR over northwest and northeast regions of India, and it is tightly correlated with CAPE over those regions. Similarly, we
 have identified three hot spots of higher lightning activity over the Indian subcontinent (Figure 1). They are located in the NEI
 (85°E - 95°E , 20°N - 30°N), NNWI (25°N - 40°N , 65°E - 80°E) and southern peninsular India (SPI) (5°N - 15°N , 75°E - 80°E).
 130 Meanwhile, the hydrometeors' variability inside convective systems develop over these regions is considered to understand
 their association with LFR. The LFR values are low during the pre-monsoon season over NNWI when the ENSO phase is
 either warm or cold (Figure 2 (a, b)). However, the same region exhibits an increase of LFR during the neutral phase (Figure 2
 (c)). While looking into the LFR anomaly of individual years, pre-monsoons of three years (1997, 1998, and 2010) have come
 under the El-Nino phase. The first two exhibits a decrease of LFR over NNWI, contributing to the overall reduction in the LFR
 135 (figure 2(a)). Out of the four La-Nina years (1999, 2000, 2008, and 2011) of pre-monsoon season, 1999, 2000 and 2011 have
 below-average values of LFR over the same region (Figure 3 (d)). The pre-monsoons of 11 years occurred during the neutral
 phase of ENSO, in which six years are showing below and five years above-average values of LFR over NNWI.

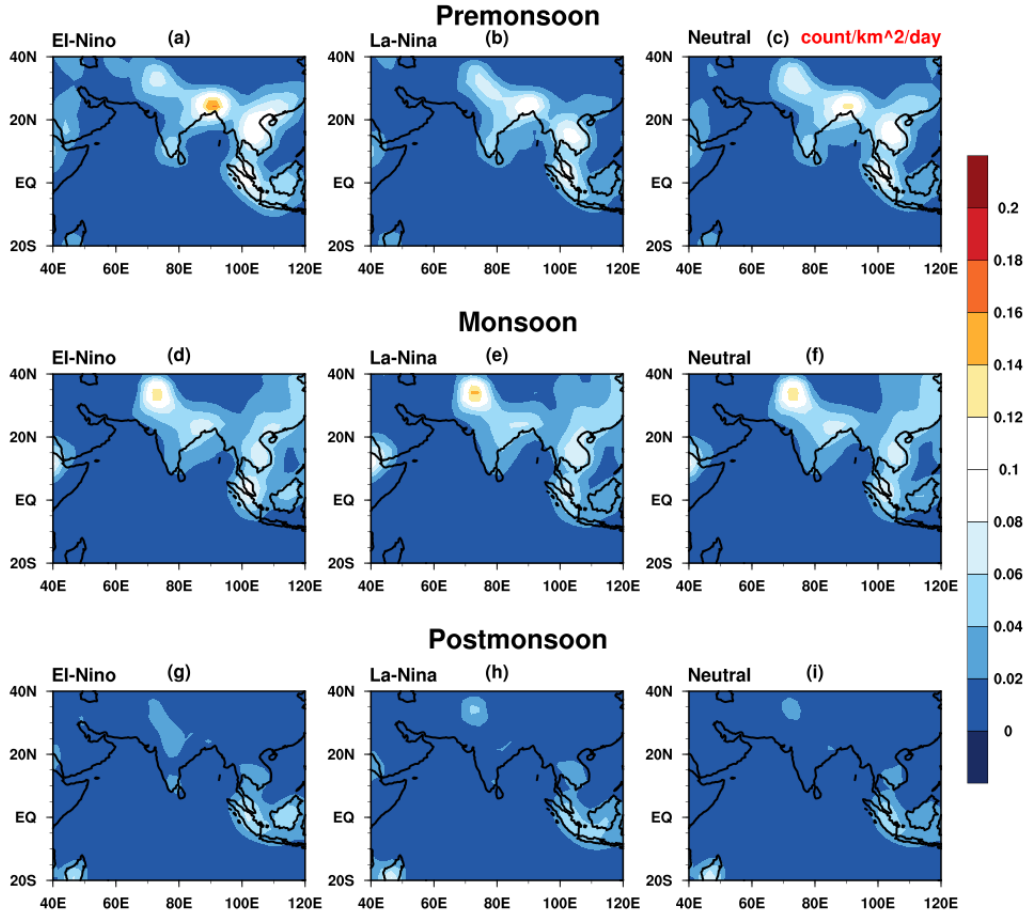


Figure 1. LFR composite during different ENSO phases.

Graupel and snow are the different forms of ice content inside the convective clouds. In situ airborne observations during the Cloud-Aerosol Interaction and Precipitation Enhancement Experiment (CAIPEEX) over various locations of India shows that convective clouds during the pre-monsoon and monsoon period have an ice water content of 10^{-4} to 1 gm^{-3} (Patade et al., 2015). Moreover, in situ measured ice cloud properties in the European Cloud Radiation Experiment (EUCREX) have reported a similar range of ice water content inside the clouds system (10^{-4} gm^{-3} to 1 gm^{-3}) (Hogan et al., 2006). From figure 6 the anomalous latent heating exists mostly between ± 0.01 . In some cases, it is extending up to ± 0.02 (Kelvin/hr); additionally, previous studies indicate these anomalous values are highly significant (Kumar et al., 2014). Linked with the decrease of

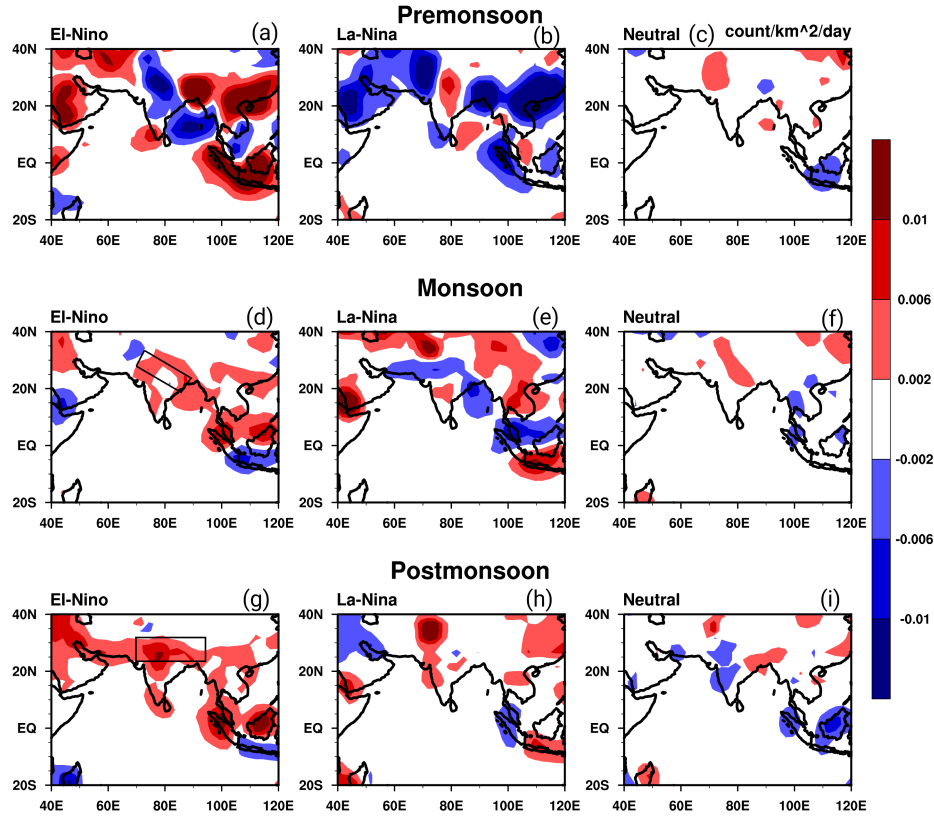


Figure 2. Anomaly composite of LFR during different ENSO phases. The box in figure (d) and (g) indicates the region of monsoon trough and western disturbance, respectively.

145 graupel and snow content over NNWI during the warm and cold phase of ENSO (Figures 4 (d), 5 (d)), latent heat (LH) release decreases (Figure 6 (d)). The anomalous negative SH at 300 hPa manifests that the clouds are unable to penetrate deep into the atmosphere during these two phases over NNWI (Figure 7 (a, b)). As a result, LFR over NNWI in these phases is low, especially in the cold phase. Contrarily, higher LFR during the neutral phase pointing the abundance of graupel and snow inside the cloud system.

150 It is noticed that ENSO warm phase during the pre-monsoon season is favourable to LFR over the NEI and SPI but unfavourable to central India (CI) (Figure 2 (a)). Conversely, the cold ENSO phase suppresses LFR over NEI and SPI with enhanced LFR over CI (Figure 2 (b)). In short, the anomalous pattern of LFR during warm and cold phases are mirror images of each other during the pre-monsoon season. Most of the regions that exhibit an increase of LFR in the warm period show decreased LFR in the cold phase of ENSO. The entire years under the cold (warm) phase during pre-monsoon are showing a

155 decrease (increase) of LFR over NEI (SPI) (Figure 3 (a, g)), which confirms that the cold phase suppresses the LFR over NEI, and the warm phase enhance it over SPI.

We display the vertical profile of graupel in figure 4 (a), which indicates that clouds over NEI have high (low) graupel content during the ENSO warm (cold) phase. An increase of snow content with a peak value near 6.5 km is also observed over NEI during pre-monsoon (Figure 5 (a)). The interaction between snow and graupel and the associated charge generation is responsible for the occurrence of lightning in convective clouds. Thus the formation of the higher (lower) amount of graupel and snow over NEI during the warm (cold) phase will release more latent heat, which is evident from figure 6 (a). Positive (negative) anomalies of SH over NEI indicates that the convective clouds formed during the ENSO warm (cold) phase are vigorous (wimpy) and consequently responsible for the enhanced (reduced) LFR. Figures 4 (g) and 5 (g) show that the graupel and snow concentrations over SPI are anomalously high up to 6 km during the cold phase of ENSO; and above that level, it decreases. This particular hydrometeor pattern reverses during the warm phase, exhibits below-average values beneath 6 km, and rapidly increases above that level. Figure 6 (g) shows the level of maximum latent heat release follows the pattern of graupel and snow concentrations. Note that the analysis presented here confirms that the warm phase of ENSO intensifies the deep convection over SPI during the pre-monsoon season and hence promotes LFR.

3.3 Distribution of anomalous LFR during monsoon season with respect to ENSO phases

The LFR over the monsoon trough region and along the northwest coast of India increases during the warm phase of ENSO (Figure 2 (d)) but remarkably decreases during the cold phase (Figure 2 (e)). Based on the 1998-1999 El-Nino event, Hamid et al. (2001) suggested that intense convective storms developing over the maritime continents are responsible for the increase of lightning activity despite a decrease in the number of convective storms. During the El-Nino years of 1997-1998 and 2002-2003, the southeast Asian regime exhibited an above-average value of lightning (Kumar and Kamra, 2012). An elongated region over central India is showing higher (lower) LFR during the warm (cold) phase of ENSO (Figure 2 (d, e)). While analysing the 300 hPa SH variability, we noticed that the amount of SH over that region is high during the warm and low during the cold phase (Figure 7 (d, e)). The NEI is showing a positive anomaly of LFR during both warm and cold phases of ENSO. Figure 3 (b) enforces this result by showcasing that all the years under the warm phase and the majority of years under the cold phase (during the monsoon season) show an increase in LFR over NEI. The similarity of LFR anomaly over NEI during the warm and cold phase is also noticeable in the vertical distribution of graupel and snow displayed in figures 4 (b) and 5 (b). In contrast, LFR is enhanced (suppressed) over NNWI during the cold (warm) period due to the presence of a larger (smaller) amount of graupel and snow. There is no noticeable change in the distribution of LFR over SPI in the three phases of ENSO (Figure 2 (d, e, f)). Further, anomalous LFR during the individual years are not showing any particular pattern corresponding to different ENSO phases over SPI (Figure 3 (h)).

It is interesting to observe that during the 12 years from 2002 to 2013, 11 years have shown above-average values of LFR over the NEI and NNWI regions (Figure 3 (b, e)), registering the intensification of deep convective cloud formation during the recent monsoon season over respective areas. Out of the nine years from 2005 to 2013, 8 have above-normal LFR over SPI (Figure 3 (h)). This indicates an escalation of deep convection over SPI in that period. Specifically, the hotspots of LFR over the Indian land region became more prominent during the last decade's monsoon seasons.

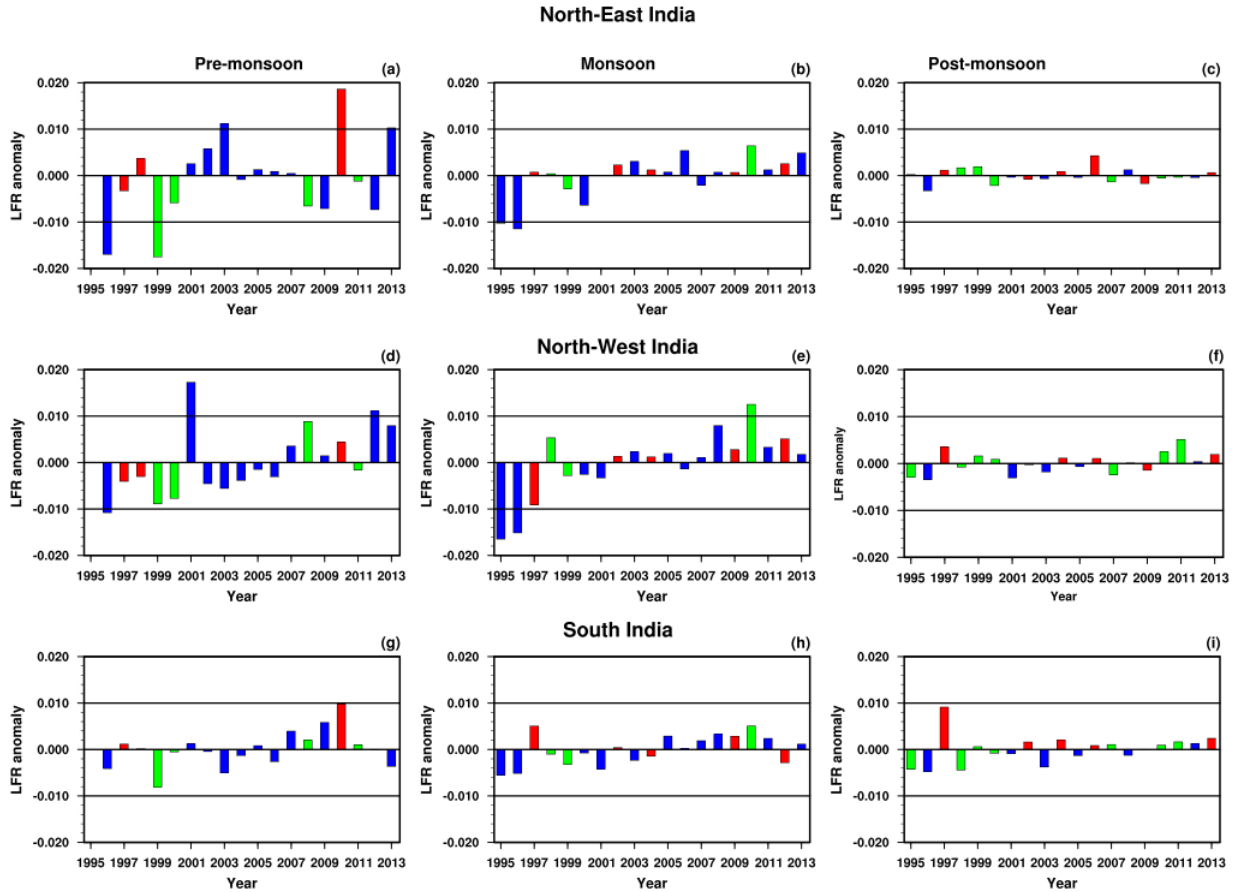


Figure 3. The anomaly of LFR during the individual years with different ENSO phases. Red color label bar corresponds to warm; green one corresponds to the cold and blue color label bar indicates the neutral phases of ENSO

190 3.4 Distribution of anomalous LFR during post-monsoon season with respect to ENSO phases

During the post-monsoon season, Western disturbances (WD), which are vertical perturbations associated with the subtropical westerly jet stream, bring rainfall to India's northern regions (Dimri et al., 2016). The jet is more intense and propagates southward during the El-Nino phase of ENSO (Schiemann et al., 2009). Our analysis shows during the post-monsoon El-Nino period, LFR is increased throughout the country and it is maximum over north-central India (Figure 2 (g)). In contrast, in the
195 cold phase, intense LFR is concentrated only over the NNWI (Figure 2 (h)). Meanwhile, NEI and NNWI are not showing any significant difference in the vertical profile of snow and graupel with different ENSO phases during the post-monsoon season (Figures 4 (c, f) and 5 (c, f)). Zubair and Ropelewski (2006) reported a significant role for ENSO in controlling the post-monsoon rainfall over SPI. The SPI is showing an increase of LFR in the warm phase of ENSO during this season due to the

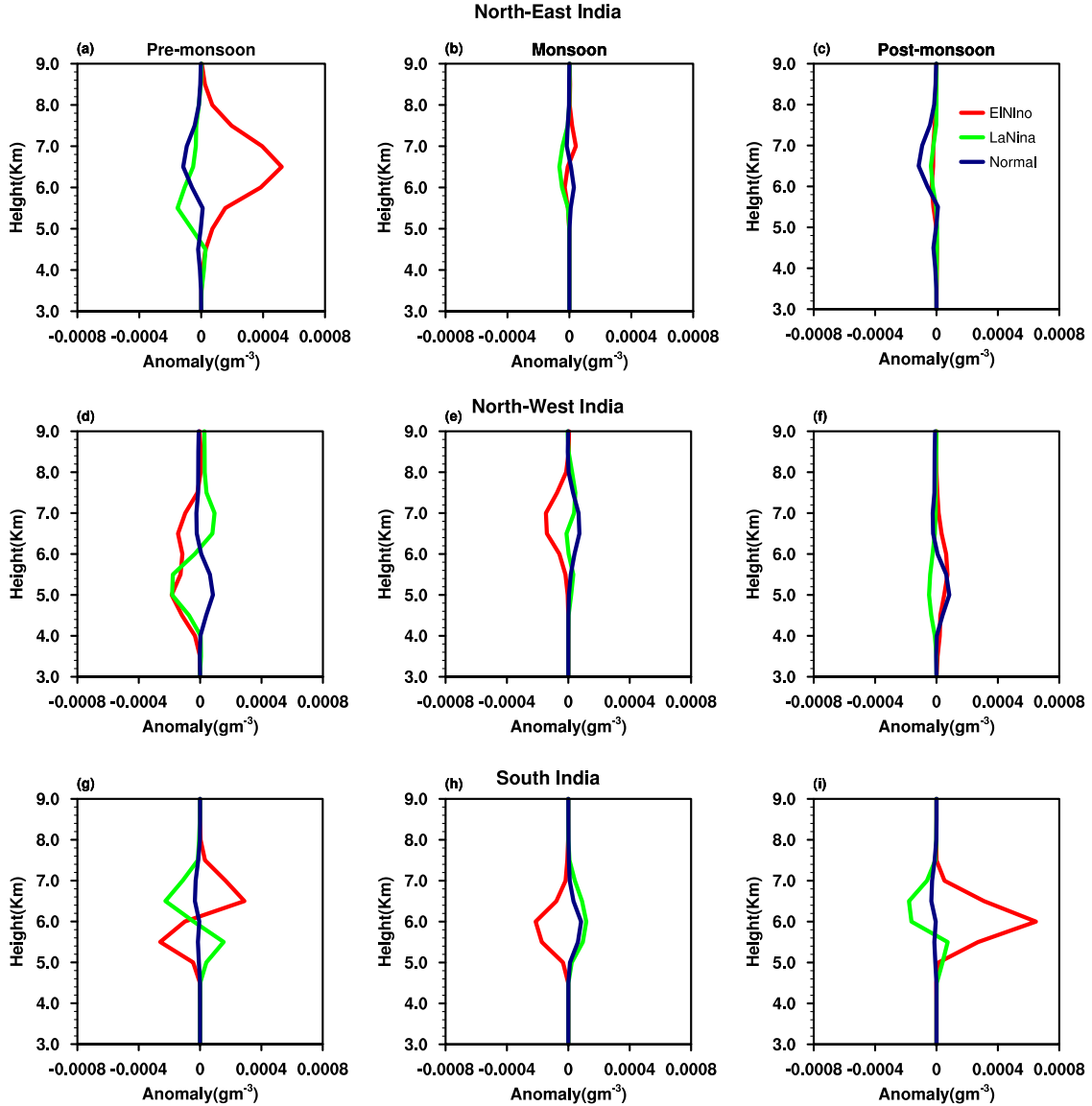


Figure 4. Anomaly composite of graupel during different ENSO phases.

presence of clouds having higher graupel and snow content over that region (Figures 2 (g), 4 (i), 5 (i)). The entire years grouped under the warm phase of ENSO during the post-monsoon season show an increase of LFR over SPI. On the other hand, during the cold phase, anomalous LFR displays an inconsistent pattern of oscillation (Figure 3 (i)). Climate variability, like ENSO, can alter the position of jet streams and hence the distribution of WD (Hunt et al., 2018). Syed et al. (2006) identified that the intensification of WDs during the El-Nino is associated with the weakening of Siberian high. Studies signify that depressions

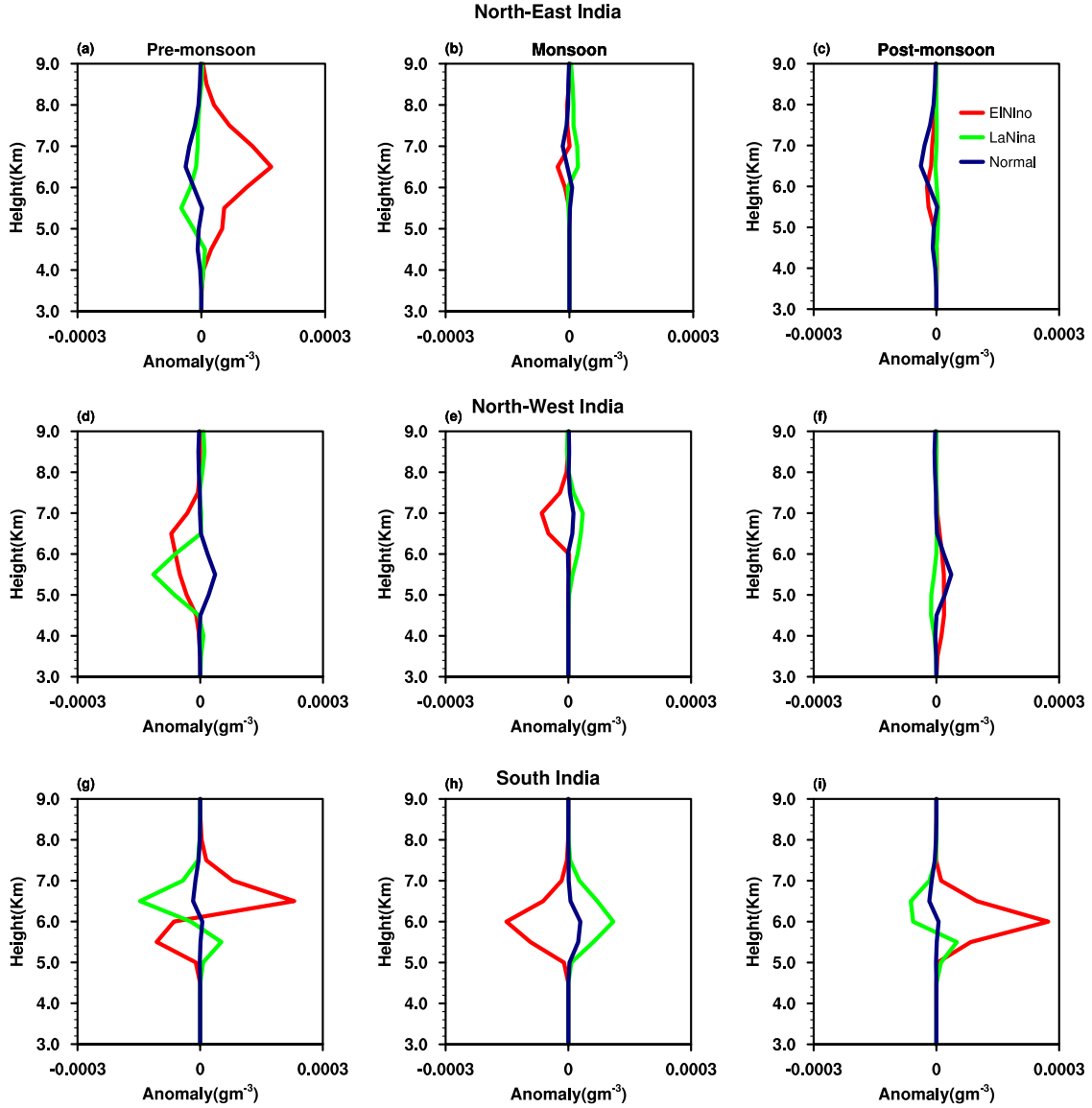


Figure 5. Composite anomaly of snow during different ENSO phases.

formed over the South Bay of Bengal and the Arabian Sea can also modulate WDs' path (Rao et al., 1969). It is exciting to note that 500 hPa GP surface drops-down (go up) from the 25°N towards the north and indicates the suppression (enhancement) of convection over that region during the warm (cold) phase of ENSO (Figure 8 (a, b)). In contrast, a higher (lower) GP surface is visible all over India during the warm (cold) phase, which is an indication of an increase (decrease) in the convective activity during the respective phases. By considering the anomalous circulation at 200 hPa level, an anomalous westerly (easterly) wind

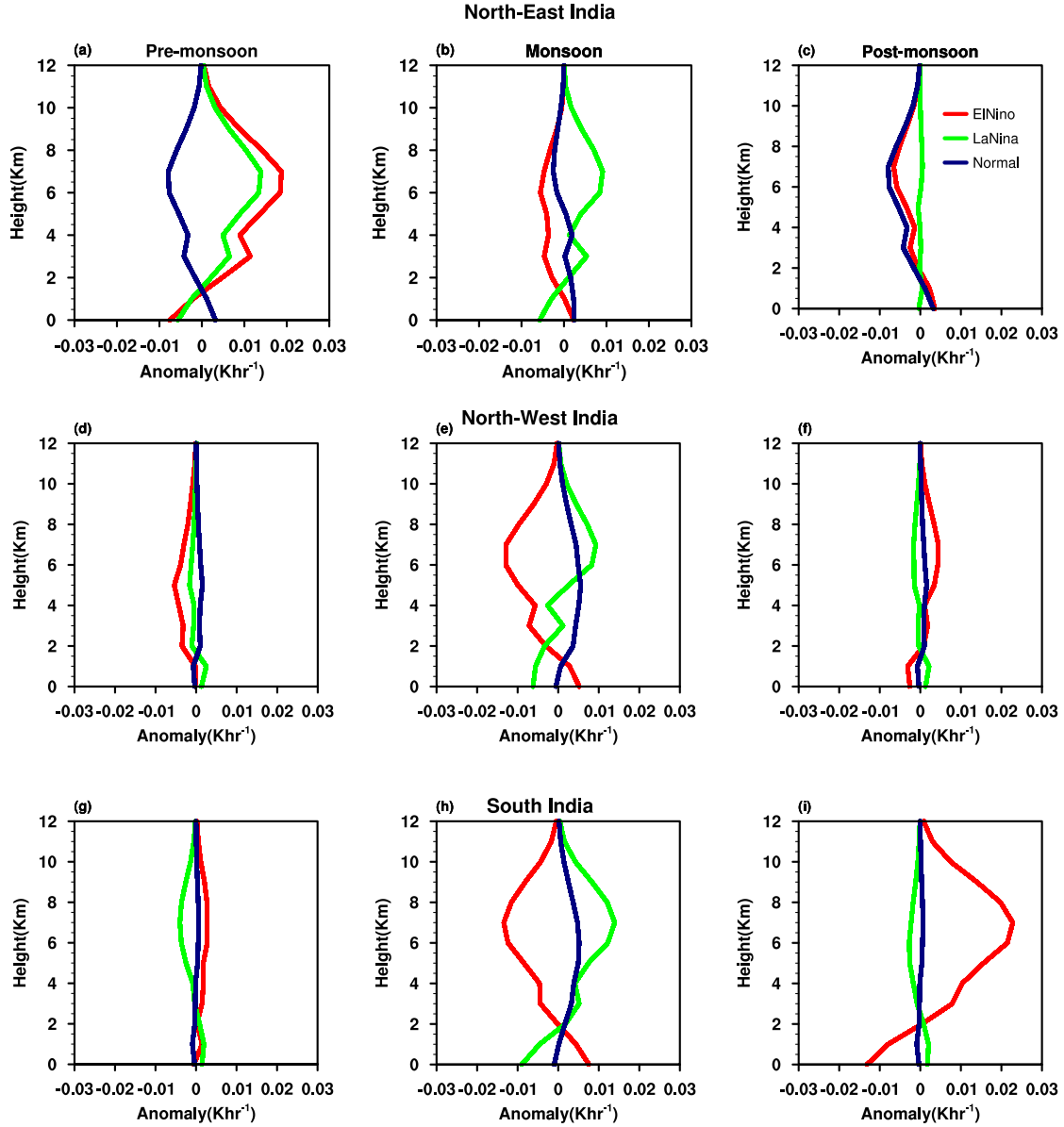


Figure 6. Composite anomaly of latent heat during different ENSO phases.

is prevalent over entire India during warm (cold) periods (Figure 8 (a, b)). Accordingly, upper-level wind pattern and variability of GPH together indicate the southward extension of WD during ENSO's warm phase. The sharp increase (decrease) of SH lies precisely over the region of the maximum undulation of GPH during the warm (cold) phase (Figure 7 (g, h)). This suggests that ENSO indirectly influences the LFR over India during the post-monsoon season by modulating WDs' path.

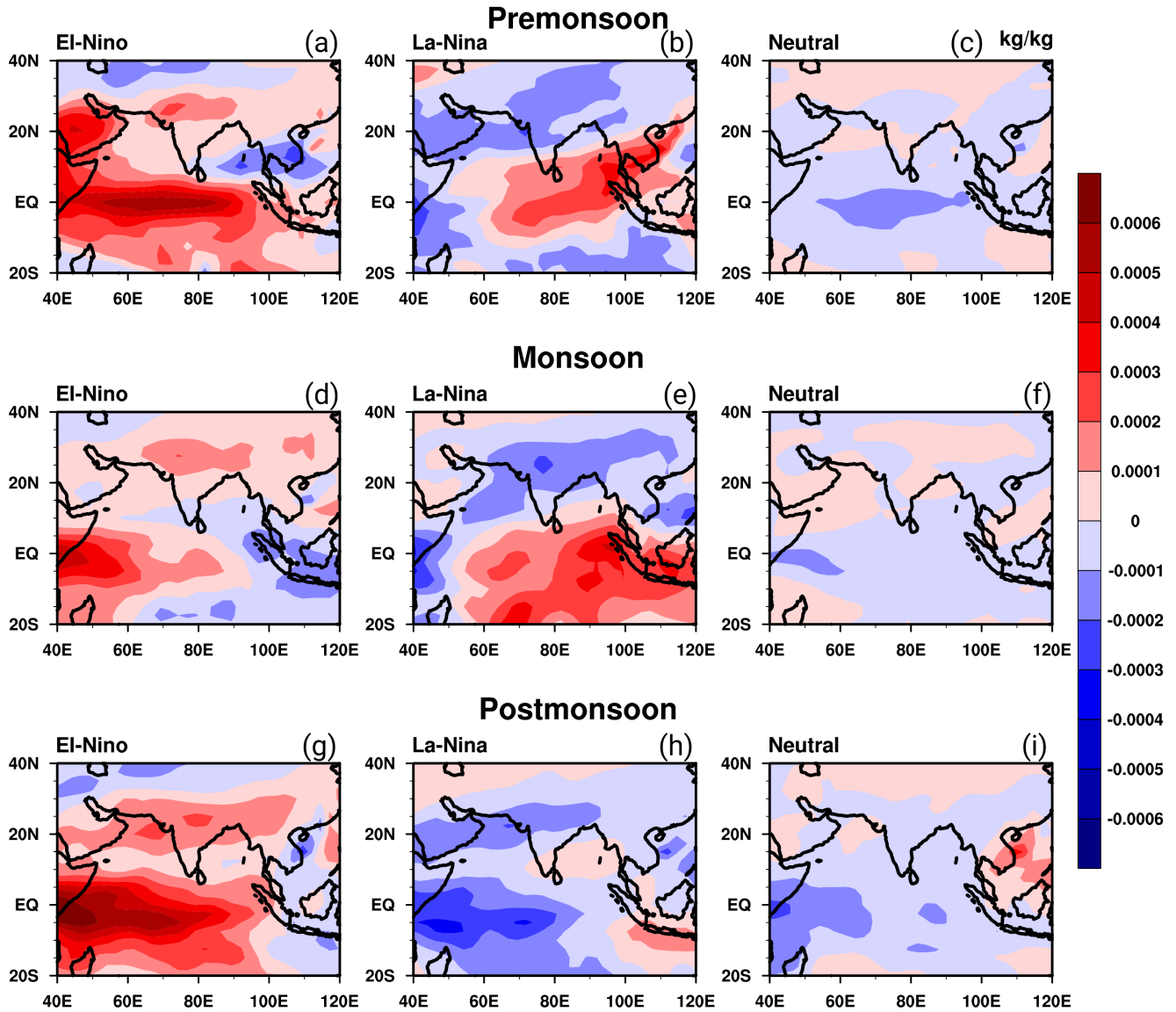


Figure 7. Anomaly composite of specific humidity at 300hPa during different ENSO phases.

4 Conclusion

In this study, we have discussed the influence of ENSO on LFR during pre-monsoon, monsoon, and post-monsoon seasons over India. Regardless of ENSO phases, the LFR is peaking at the time of pre-monsoon season over NEI and SPI. However, the NNWI exhibits a peak LFR during the monsoon season. The LFR is increased (decreased) over NEI and SPI during the

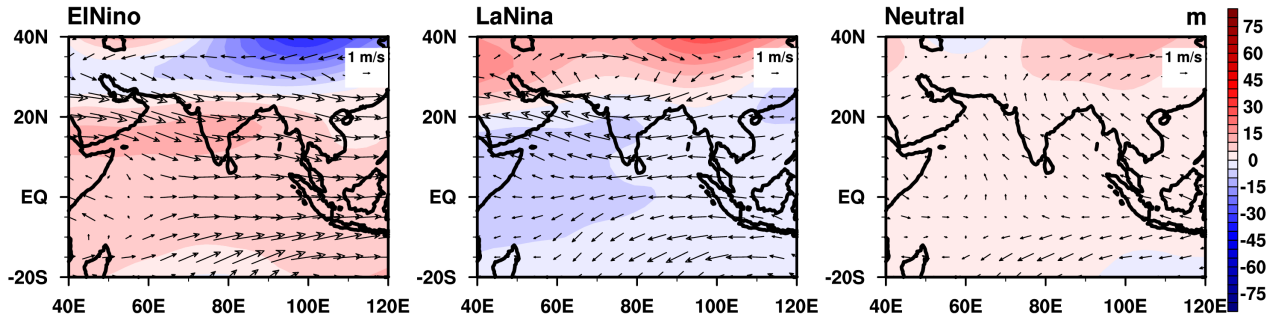


Figure 8. Anomaly composite of geopotential height at 500hPa and 200hPa wind during different ENSO phases.

warm (cold) phase of ENSO, and anomalies of the charge generating hydrometeors show a similar kind of swing. Furthermore, the entire years under the cold (warm) phase during the pre-monsoon season taken in this study is characterized by a decrease (increase) of LFR over NEI (SPI), which firmly indicates that the cold phase suppresses the LFR over NEI, and the warm phase enhance it over SPI.

During the cold phase in pre-monsoon, graupel and snow concentration over SPI shows an above-average value up to 6 km. This particular pattern of these hydrometeors reverses during the warm phase. The increase in graupel and snow formation above 6 km pinpoint that the warm phase of ENSO is conducive for deep convection over SPI during the pre-monsoon and hence higher LFR. However, the neutral phase of ENSO favours deepening of clouds over NNWI, as evidenced by the high values of the upper level-specific humidity. At the time of monsoon season, LFR over NEI is high during both El-Nino and La-Nina periods. Over NNWI, LFR increases during La-Nina but diminishes during El-Nino. The SPI does not show significant variation in LFR with respect to different ENSO phases during the monsoon season. While considering the recent 12 years of this study, irrespective of the ENSO phases, every year has displayed above-average values of LFR over the NEI and NNWI region. Out of 9 years from 2005 to 2013, 8 displayed above-normal LFR over SPI, which signifies the intensification of LFR over the three hotspots in the last decades of the monsoon season. Almost all regions in India are exhibiting higher LFR during the warm ENSO phase in the post-monsoon season. The elevated (reduced) GPH is visible all over India during the warm (cold) phase of ENSO, which is an indication of an increase (decrease) in the convective activity during the respective phases. The entire years grouped under the warm phase of ENSO during the post-monsoon season show an increase of LFR over SPI, whereas the years elected under the cold phase shows a disperse anomalous pattern. Both intensification and southward extension of WD is responsible for higher LFR over India in the warm phase, indicating indirect interaction between ENSO and LFR by modulating the mid-latitude westerlies.

Data availability. The LIS/OTD data and vertical profiles of hydrometeors, and latent heat obtained from the website <http://ghrc.nsstc.nasa.gov/> and <https://disc.gsfc.nasa.gov/datasets/> respectively. The GPH, wind and SH data are available the weblink <https://psl.noaa.gov/data/gridded/data.ncep.reanalysis.html>. The HadISST data used in this work is accessible from the weblink https://psl.noaa.gov/gcos_wgsp/.

Author contributions. The paper and its methodology were conceptualized and developed by SA, AVS, and PV; AVS performed the analyses, and PV curated the data. The original draft preparation was by AVS; further reviewing and editing was by PV and SA. AVS handled visualization.

240 *Competing interests.* The authors declare that they have no known competing financial interests or personal relationships that could have appeared to influence the work reported in this paper.

Acknowledgements. We are grateful to NASA and PSL for providing LIS/ODT, TRMM, and NCEP Reanalysis data products, respectively, which are used in this study. Sreenath A V acknowledges Kerala State Council for Science, Technology, and Environment (KSCSTE), India, for providing financial support. Support from the Department of Atmospheric Sciences, Cochin University of Science and Technology is
245 acknowledged.

References

- Ahmad, A. and Ghosh, M.: Variability of lightning activity over India on ENSO time scales, *Advances in Space Research*, 60, 2379–2388, 2017.
- Blakeslee, R. J., Mach, D. M., Bateman, M. G., and Bailey, J. C.: Seasonal variations in the lightning diurnal cycle and implications for the
250 global electric circuit, *Atmospheric research*, 135, 228–243, 2014.
- Cecil, D. J., Buechler, D. E., and Blakeslee, R. J.: Gridded lightning climatology from TRMM-LIS and OTD: Dataset description, *Atmospheric Research*, 135, 404–414, 2014.
- Cess, R. D., Zhang, M., Wielicki, B. A., Young, D. F., Zhou, X.-L., and Nikitenko, Y.: The influence of the 1998 El Niño upon cloud-radiative forcing over the Pacific warm pool, *Journal of climate*, 14, 2129–2137, 2001.
- 255 Christian, H. J., Blakeslee, R. J., Boccippio, D. J., Boeck, W. L., Buechler, D. E., Driscoll, K. T., Goodman, S. J., Hall, J. M., Koshak, W. J., Mach, D. M., et al.: Global frequency and distribution of lightning as observed from space by the Optical Transient Detector, *Journal of Geophysical Research: Atmospheres*, 108, ACL–4, 2003.
- Chronis, T., Goodman, S., Cecil, D., Buechler, D., Robertson, F., Pittman, J., and Blakeslee, R.: Global lightning activity from the ENSO perspective, *Geophysical Research Letters*, 35, 2008.
- 260 Cooray, V., Rakov, V., and Theethayi, N.: The lightning striking distance—Revisited, *Journal of Electrostatics*, 65, 296–306, 2007.
- Dimri, A., Yasunari, T., Kotlia, B., Mohanty, U., and Sikka, D.: Indian winter monsoon: Present and past, *Earth-science reviews*, 163, 297–322, 2016.
- Goodman, S., Buechler, D., Knupp, K., Driscoll, K., and McCaul Jr, E.: The 1997–98 El Niño event and related wintertime lightning variations in the southeastern United States, *Geophysical Research Letters*, 27, 541–544, 2000.
- 265 Goodman, S., Buechler, D., and McCaul, E.: Lightning, in *Our Changing Planet: The View From Space*, 44–52, 2007.
- Goswami, B. B., Mukhopadhyay, P., Mahanta, R., and Goswami, B.: Multiscale interaction with topography and extreme rainfall events in the northeast Indian region, *Journal of Geophysical Research: Atmospheres*, 115, 2010.
- Hamid, E. Y., Kawasaki, Z.-I., and Mardiana, R.: Impact of the 1997–98 El Niño event on lightning activity over Indonesia, *Geophysical Research Letters*, 28, 147–150, 2001.
- 270 Hogan, R. J., Mittermaier, M. P., and Illingworth, A. J.: The retrieval of ice water content from radar reflectivity factor and temperature and its use in evaluating a mesoscale model, *Journal of Applied Meteorology and Climatology*, 45, 301–317, 2006.
- Houze Jr, R. A., Wilton, D. C., and Smull, B. F.: Monsoon convection in the Himalayan region as seen by the TRMM Precipitation Radar, *Quarterly Journal of the Royal Meteorological Society: A journal of the atmospheric sciences, applied meteorology and physical oceanography*, 133, 1389–1411, 2007.
- 275 Hsu, C.-P. F. and Wallace, J. M.: The global distribution of the annual and semiannual cycles in precipitation, *Monthly Weather Review*, 104, 1093–1101, 1976.
- Hunt, K. M., Turner, A. G., and Shaffrey, L. C.: The evolution, seasonality and impacts of western disturbances, *Quarterly Journal of the Royal Meteorological Society*, 144, 278–290, 2018.
- Kamra, A. and Athira, U.: Evolution of the impacts of the 2009–10 El Niño and the 2010–11 La Niña on flash rate in wet and dry environments
280 in the Himalayan range, *Atmospheric Research*, 182, 189–199, 2016.
- Kandalgaonkar, S., Kulkarni, J., Tinmaker, M., and Kulkarni, M.: Land-ocean contrasts in lightning activity over the Indian region, *International Journal of Climatology: A Journal of the Royal Meteorological Society*, 30, 137–145, 2010.

- Kent, G., Williams, E., Wang, P., McCormick, M., and Skeens, K.: Surface temperature related variations in tropical cirrus cloud as measured by SAGE II, *Journal of Climate*, 8, 2577–2594, 1995.
- 285 Kilinc, M. and Beringer, J.: The spatial and temporal distribution of lightning strikes and their relationship with vegetation type, elevation, and fire scars in the Northern Territory, *Journal of climate*, 20, 1161–1173, 2007.
- Kulkarni, M. and Siingh, D.: The relation between lightning and cosmic rays during ENSO with and without IOD—a statistical study, *Atmospheric Research*, 143, 129–141, 2014.
- Kumar, P. R. and Kamra, A.: Variability of lightning activity in South/Southeast Asia during 1997–98 and 2002–03 El Nino/La Nina events, 290 *Atmospheric research*, 118, 84–102, 2012.
- Kumar, S., Hazra, A., and Goswami, B.: Role of interaction between dynamics, thermodynamics and cloud microphysics on summer monsoon precipitating clouds over the Myanmar Coast and the Western Ghats, *Climate dynamics*, 43, 911–924, 2014.
- Lau, K.-M., Ramanathan, V., Wu, G.-X., Li, Z., Tsay, S., Hsu, C., Sikka, R., Holben, B., Lu, D., Tartari, G., et al.: The Joint Aerosol–Monsoon Experiment: A new challenge for monsoon climate research, *Bulletin of the American Meteorological Society*, 89, 369–384, 2008.
- 295 Mills, B., Unrau, D., Pentelow, L., and Spring, K.: Assessment of lightning-related damage and disruption in Canada, *Natural hazards*, 52, 481–499, 2010.
- Murugavel, P., Pawar, S., and Gopalakrishnan, V.: Climatology of lightning over Indian region and its relationship with convective available potential energy, *International Journal of Climatology*, 34, 3179–3187, 2014.
- Patade, S., Prabha, T., Axisa, D., Gayatri, K., and Heymsfield, A.: Particle size distribution properties in mixed-phase monsoon clouds from 300 in situ measurements during CAIPEEX, *Journal of Geophysical Research: Atmospheres*, 120, 2015.
- Petersen, W. A., Rutledge, S. A., and Orville, R. E.: Cloud-to-ground lightning observations from TOGA COARE: Selected results and lightning location algorithms, *Monthly weather review*, 124, 602–620, 1996.
- Rao, Y., Srinivasan, V., Raman, S., and RAMAKRISHNAN, A.: Forecasting manual, Part-II, Discussion of typical synoptic weather situation, winter-western disturbances and their associated features. FMU Report No. III-1.1, India Meteorological Department. Delhi, India, 1969.
- 305 Rasmussen, K. L. and Houze Jr, R. A.: Orographic convection in subtropical South America as seen by the TRMM satellite, *Monthly Weather Review*, 139, 2399–2420, 2011.
- Romatschke, U., Medina, S., and Houze Jr, R. A.: Regional, seasonal, and diurnal variations of extreme convection in the South Asian region, *Journal of climate*, 23, 419–439, 2010.
- Rosenfeld, D.: TRMM observed first direct evidence of smoke from forest fires inhibiting rainfall, *Geophysical research letters*, 26, 3105–3108, 1999. 310
- Sátori, G., Williams, E., and Lemperger, I.: Variability of global lightning activity on the ENSO time scale, *Atmospheric Research*, 91, 500–507, 2009.
- Schiemann, R., Lüthi, D., and Schär, C.: Seasonality and interannual variability of the westerly jet in the Tibetan Plateau region, *Journal of Climate*, 22, 2940–2957, 2009.
- 315 Selvi, S. and Rajapandian, S.: Analysis of lightning hazards in India, *International Journal of Disaster Risk Reduction*, 19, 22–24, 2016.
- Singh, O. and Singh, J.: Lightning fatalities over India: 1979–2011, *Meteorological Applications*, 22, 770–778, 2015.
- Syed, F., Giorgi, F., Pal, J., and King, M.: Effect of remote forcings on the winter precipitation of central southwest Asia part 1: observations, *Theoretical and Applied Climatology*, 86, 147–160, 2006.
- Takahashi, T., Tajiri, T., and Sono, Y.: Charges on graupel and snow crystals and the electrical structure of winter thunderstorms, *Journal of the atmospheric sciences*, 56, 1561–1578, 1999. 320

- Tinmaker, M., Aslam, M., and Chate, D.: Lightning activity and its association with rainfall and convective available potential energy over Maharashtra, India, *Natural Hazards*, 77, 293–304, 2015.
- Venevsky, S.: Importance of aerosols for annual lightning production at global scale., *Atmospheric Chemistry & Physics*, 14, 2014.
- Williams, E., Rosenfeld, D., Madden, N., Gerlach, J., Gears, N., Atkinson, L., Dunnemann, N., Frostrom, G., Antonio, M., Biazon, B., et al.:
325 Contrasting convective regimes over the Amazon: Implications for cloud electrification, *Journal of Geophysical Research: Atmospheres*, 107, LBA–50, 2002.
- Williams, E. R.: The Schumann resonance: A global tropical thermometer, *Science*, 256, 1184–1187, 1992.
- Williams, E. R.: The electrification of severe storms, in: *Severe Convective Storms*, pp. 527–561, Springer, 2001.
- Williams, E. R., Geotis, S., Renno, N., Rutledge, S., Rasmussen, E., and Rickenbach, T.: A radar and electrical study of tropical “hot towers”,
330 *Journal of the atmospheric sciences*, 49, 1386–1395, 1992.
- Yadava, P. K., Soni, M., Verma, S., Kumar, H., Sharma, A., and Payra, S.: The major lightning regions and associated casualties over India, *Natural Hazards*, 101, 217–229, 2020.
- Yang, S., Lau, K., and Kim, K.: Variations of the East Asian jet stream and Asian–Pacific–American winter climate anomalies, *Journal of Climate*, 15, 306–325, 2002.
- 335 Zipser, E. J.: Deep cumulonimbus cloud systems in the tropics with and without lightning, *Monthly weather review*, 122, 1837–1851, 1994.
- Zipser, E. J., Cecil, D. J., Liu, C., Nesbitt, S. W., and Yorty, D. P.: Where are the most intense thunderstorms on Earth?, *Bulletin of the American Meteorological Society*, 87, 1057–1072, 2006.
- Zubair, L. and Ropelewski, C. F.: The strengthening relationship between ENSO and northeast monsoon rainfall over Sri Lanka and southern India, *Journal of Climate*, 19, 1567–1575, 2006.